Testosterone-loaded GM1 micelles targeted to the intracellular androgen receptor for the specific induction of genomic androgen signaling

Nahuel Peinetti, Mariana Micaela Cuello Rubio, Liliana Del Valle Sosa, María Victoria Scalerandi, Roxana Valeria Alasino, Victoria Peyret, Juan Pablo Nicola, Dante Miguel Beltramo, Amado Alfredo Quintar, Cristina Alicia Maldonado

PII: S0378-5173(20)30970-4
DOI: https://doi.org/10.1016/j.ijpharm.2020.119985
Reference: IJP 119985

To appear in: *International Journal of Pharmaceutics*

Received Date: 2 June 2020
Revised Date: 8 October 2020
Accepted Date: 11 October 2020

Please cite this article as: N. Peinetti, M. Micaela Cuello Rubio, L. Del Valle Sosa, M. Victoria Scalerandi, R. Valeria Alasino, V. Peyret, J. Pablo Nicola, D. Miguel Beltramo, A. Alfredo Quintar, C. Alicia Maldonado, Testosterone-loaded GM1 micelles targeted to the intracellular androgen receptor for the specific induction of genomic androgen signaling, *International Journal of Pharmaceutics* (2020), doi: https://doi.org/10.1016/j.ijpharm.2020.119985

Testosterone-loaded GM1 micelles targeted to the intracellular androgen receptor for the specific induction of genomic androgen signaling

Nahuel Peinetti[a,b], Mariana Micaela Cuello Rubio[a,b], Liliana Del Valle Sosa[a,b], María Victoria Scalerandi[a,b], Roxana Valeria Alasino[c,d], Victoria Peyret[e,f], Juan Pablo Nicola[e,f], Dante Miguel Beltramo[c,d,g], Amado Alfredo Quintar[a,b,# *], Cristina Alicia Maldonado[a,b,#]

[a] *Universidad Nacional de Córdoba, Facultad de Ciencias Médicas, Centro de Microscopía Electrónica. Córdoba, Argentina.*

[b] *Consejo Nacional de Investigaciones Científicas y Técnicas (CONICET), Instituto de Investigaciones en Ciencias de la Salud (INICSA), Córdoba, Argentina.*

[c] *Gobierno de la Provincia de Córdoba, Centro de Excelencia en Productos y Procesos de Córdoba (CEPROCOR), Santa María de Punilla, Argentina.*

[d] *Consejo Nacional de Investigaciones Científicas y Técnicas (CONICET), Buenos Aires, Argentina.*

[e] *Universidad Nacional de Córdoba, Facultad de Ciencias Químicas, Departamento de Bioquímica Clínica, Córdoba, Argentina.*

[f] *Consejo Nacional de Investigaciones Científicas y Técnicas (CONICET), Centro de Investigaciones en Bioquímica Clínica e Inmunología (CIBICI), Córdoba, Argentina.*

[g] *Universidad Católica de Córdoba, Facultad de Ciencias Químicas, Cátedra de Biotecnología, Córdoba, Argentina.*

[#] *Both authors have contributed equally to this work*

***Corresponding author**: Amado Quintar, MD PhD. Centro de Microscopia Electrónica. INICSA-CONICET. Facultad de Ciencias Médicas. Universidad Nacional de Córdoba. Pabellón de Biología Celular 1° piso. Bv. De la Reforma and Enfermera Gordillo. Ciudad

Universitaria. 5000 Córdoba, Argentina. Phone: +54 0351-4333021 Email: aquintar@cmefcm.uncor.edu

Conflict of Interest: The authors have declared that no conflict of interest exists.

Abstract

Androgens play a central role in homeostatic and pathological processes of the prostate gland. At the cellular level, testosterone activates both the genomic signaling pathway, through the intracellular androgen receptor (AR), and membrane-initiated androgen signaling (MIAS), by plasma membrane receptors. We have previously shown that the activation of MIAS induces uncontrolled proliferation and fails to stimulate the beneficial immunomodulatory effects of testosterone in prostatic cells, becoming necessary to investigate if genomic signaling mediates homeostatic effects of testosterone. However, the lack of specific modulators for genomic androgen signaling has delayed the understanding of this mechanism. In this article, we demonstrate that monosialoganglioside (GM1) micelles are capable of delivering testosterone into the cytoplasm to specifically activate genomic signaling. Stimulation with testosterone-loaded GM1 micelles led to the activation of androgen response element (ARE)-regulated genes *in vitro* as well as to the recovery of normal prostate size and histology after castration in mice. In addition, these micelles avoided MIAS, as demonstrated by the absence of rapid signaling pathway activation and the inability to induce uncontrolled cell proliferation. In conclusion, our results validate a novel tool for the specific activation of genomic androgen signaling and demonstrate the importance of selective pathway activation in androgen-mediated proliferation.

Keywords

Testosterone; Membrane-Initiated Androgen Signaling (MIAS); Nanoparticles; Monosialoganglioside (GM1); Prostate; Genomic Androgen Signaling; Androgen Receptor (AR)

1. Introduction

Androgen signaling plays an important role in all aspects of the prostate gland. Its actions include organ development, maintenance of homeostasis during adulthood, and activation of proliferative pathways, which are critical for the progression of benign prostatic hyperplasia (BPH) and prostate cancer (PCa) [1-3]. Accordingly, there are several mechanisms of androgen signaling that can be activated at cellular level; substantial differences between them can be found on the type of receptor involved. In one hand, the androgen receptor (AR) binds to its ligand in the cytoplasm and subsequently migrates into the nucleus to behave as a ligand-activated transcription factor to induce genomic androgen signaling [4]. Alternatively, androgens can also bind to different types of plasma membrane receptors to activate Membrane-Initiated Androgen Signaling (MIAS), that acts through transduction pathways and alternative transcription factors [5,6]. We have previously evidenced that MIAS activation induces uncontrolled cell proliferation, which could be associated with proliferative prostate malignancies [7]. Moreover, MIAS is unable to reproduce the beneficial immunomodulatory effects of testosterone that have been proven important in different models of prostatitis and BPH [7-10]. These promising results show the potential advantages of agonists that can specifically target genomic androgen signaling. Although selective modulators of MIAS have been available for some time [11,12], the development of specific activators of intracellular ARs has been an unsuccessful task.

The precise delivery of substances into the cytosolic compartment of the cell has been one of the great accomplishments of nanotechnology [13,14]. Different types of loaded nanoparticles can be internalized through endocytic or non-endocytic pathways to subsequently release their content into the cytoplasm [15,16]. For instance, monosialoganglioside (GM1) micelles are able to encapsulate hydrophobic molecules in their

interior to release them inside the cell [17,18]. Many advantages have already been shown for this system in the delivery of drugs such as paclitaxel, docetaxel, amphotericin B, and doxorubicin [18-20]. GM1 micellar structures show considerable benefits as compared to other nanoparticles. Particularly, due to their small size, GM1 micelles avoid a quick removal by the reticuloendothelial system, and due to a very low critical micellar concentration (CMC), this micelles are stable at very low concentrations [17].

In this article we have validated a novel strategy to specifically activate the intracellular AR-mediated genomic signaling, while avoiding the pathogenic effects of MIAS by delivering testosterone into the cytoplasm using GM1 micelles.

2. Materials and Methods

2.1. Preparation and characterization of testosterone-loaded GM1 micelles

Testosterone-loaded GM1 micelles (GM1-T) were prepared prior to use, 0.1 ml of $1x10^{-3}$M testosterone (Sigma-Aldrich, St. Louis, MO) in DMSO (Sigma-Aldrich) was added to 1 ml of 50 mg/ml GM1 (Sinaxial™, TRB Pharma, Buenos Aires, Argentina), slowly mixed with gentle agitation and allowed to stand for 2 hours. Then, the preparation was dialyzed against PBS to remove the excess of DMSO and free testosterone.

The size and morphology of the micelles were analyzed by Transmission Electron Microscopy (TEM), using a LEO906E electron microscope (Zeiss, Oberkochen, Germany) and photographed with a Megaview III camera (Olympus, Center Valley, PA). Briefly, a solution of vehicle- or testosterone-loaded GM1 micelles was diluted 1:100 in PBS. For negative staining, 20 µl of the sample were mixed with 20 µl of 2% phosphotungstic acid in ultra-pure water. Immediately after, a drop of this mixture was placed on parafilm and a formvar-coated grid for TEM was placed on top for 20 minutes. To study the effects of pH on micellar size, GM1-T micelles were diluted 1:100 in one of the following buffers: 0.1 M Citrate buffer (pH 3), 0.1 M Citrate buffer (pH 5), 0.1 M PBS (pH 7,) or 0.1 M Carbonate buffer (pH 10). In this case, 20 µl of the sample were incubated with a formvar-coated grid for 20 minutes, washed 5 times for 1 minute each with ultra-pure water and incubated for 8 minutes with phosphotungstic acid. To determine the size of the particles, 3000 micelles were measured per sample using Image J software (NIH, Bethesda, MD).

The average particle size of empty or loaded micelles was also measured by dynamic light scattering (DLS) performed on a Delsa™ Nano Submicron Particle Size and Zeta Potential Particle Analyzer (Beckman Coulter, Inc., Brea, CA) at a fixed scattering angle of

165°. Data were analyzed by Delsa Nano Beckman Coulter software (version 2.2) with CONTIN analysis method.

2.2. Size exclusion chromatography

Micelles were analyzed on an Åkta Explorer 100 FPLC system (GE Healthcare, Chicago, IL) fitted with a Superdex 200 column, previously equilibrated with 50 mM phosphate buffer (pH 7) and 150 mM NaCl at a rate of 0.4 ml min^{-1}. The elution profile was followed using a UV-detector at 227 nm.

2.3. Preparation of fluorescent testosterone ($T_{\lambda 600}$) and GM1-$T_{\lambda 600}$

The preparation of $T_{\lambda 600}$ was adapted from protocols described elsewhere [21,22]. Briefly, 422 µl of sulfuric acid were mixed with 228 µl of ethanol and later added to 8.5 µl of testosterone $1x10^{-3}$ M previously diluted in DMSO. The solution was heated at 85ºC for 10 minutes and then cooled on ice for 3 minutes. After this, 325 µl of ethanol were added and the solution was again chilled on ice for 10 seconds. Before use, the solution was kept protected from light for an extra 30 minutes at 4ºC. The emission spectrum was calculated by exciting the sample with 570nm wavelength, with the emission being measured from 570 to 700 nm in a LV1200 CLSM (Olympus, Tokyo Japan). For GM1-$T_{\lambda 600}$ preparation, $T_{\lambda 600}$ was loaded into GM1 micelles using the same procedure used for testosterone.

2.4. Determination of the efficiency of GM1 micelles to retain testosterone

GM1-T or GM1-$T_{\lambda 600}$ micelles, prepared as explained in section 2.1 and 2.3 respectively, were dialyzed with agitation at room temperature against 10 times the volume of PBS using a dialysis membrane with a cut-off of 12kDa (Sigma-Aldrich). After 1 or 2

hours, samples of the solution were recovered. Testosterone was quantified by Electrochemiluminescence immunoassay (ECLIA) using the Elecsys Testosterone II kit and analyzed by a Cobas e411 analyzer (Roche Diagnostics, Risch-Rotkreuz, Switzerland), while $T_{\lambda 600}$ was quantified by fluorescence emission using a Glomax-Multi Detection System (Promega, Madison, WI).

2.5. Animals

Male Wistar rats and Albino Swiss mice were housed at the Animal Research Facility of the INICSA-CONICET, Córdoba, Argentina. Animal care and procedures were conducted following the guidelines of the National Institutes of Health for the care and use of laboratory animals and approved by the committee for the care and use of experimental animals of the School of Medicine, National University of Córdoba.

2.6. Human samples

Human prostate samples were obtained from four patients with BPH undergoing transurethral resection of the prostate (TURP) at the Sanatorio Allende (Córdoba, Argentina). All procedures were approved by the Ethics Committee of the Sanatorio Allende and performed under informed written consent of the patients.

2.7. Cell cultures and treatments

The human prostatic LNCaP cell line was kindly provided by Dr. Elba Vazquez (IQUIBICEN-CONICET) and was used at passage numbers 36-42. Cells were cultured in MCDB medium (Sigma-Aldrich) containing 15% of fetal calf serum (FCS) (Internegocios, Buenos Aires, Argentina).

Primary cultures of rat prostate stromal cells (rPSC) were done as previously described [23]. Briefly, ventral prostates from adult (3 months) Wistar rats were removed, minced into small fragments, and treated with a digestion solution containing 200 U/ml of collagenase type IA (Sigma-Aldrich) in MCDB131 medium (Sigma-Aldrich) for 30 minutes. Cells were then seeded in 6-well culture plates at a density of $7.5x10^5$ cells per well and cultured in MCDB131 containing 15% FCS.

For primary cultures of human prostatic stromal cell (HPSC), prostate biopsies were placed on ice-cold MCDB131 medium for transportation to the laboratory. Samples were then minced into small fragments and treated with digestion solution of 200 U/ml collagenase type IA in MCDB131 medium for 3 hours. Cells were seeded in 6 well plates and grown for a minimum of 15 days in MCDB131 supplemented with 15% FCS. Then, cells were split for at least 6 passages before protocols in order to ensure the stromal purity of the cultures. The stromal cell phenotype was checked by immunocytochemistry of calponin, alpha-smooth muscle actin, and vimentin as described before (data not shown) [24].

All cells (primary cultures and cell lines) were grown in a humidified incubator at 37°C supplied with 5% CO_2. Culture media were supplemented with penicillin and streptomycin and was replaced every two days. Previous to the stimuli, cells were grown in serum-free MCDB131 medium supplemented with 5 mg/ml insulin (Sigma-Aldrich), 5 mg/ml transferrin (Sigma-Aldrich), 5 ng/ml selenite (Sigma-Aldrich) for 24 hours. The following drugs and concentrations were used for stimuli: testosterone ($1x10^{-8}$ M), GM1 ($1x10^{-6}$ M)-T ($1x10^{-8}$ M), testosterone-bovine serum albumin conjugate (T-BSA) ($1x10^{-8}$ M, Sigma-Aldrich) for the specific activation of MIAS, or their vehicles. Cells were stimulated for 30 or 60 minutes for phosphorylation assays, 8 hours for qPCR and 24 hours for proliferation assays. To determine AR expression, cells were stimulated for 24 hours with

different concentrations of testosterone or GM1 ($1x10^{-6}$ M)-T. For viability assay, cells were stimulated with different doses of GM1 (0.005-500 µg/ml) for 24 hours and counted under a Neubauer chamber. A 10% v/v Trypan Blue (Sigma-Aldrich) solution was used to discard dead cells.

2.8. Confocal Laser Scanning Microscopy Analysis

LNCaP cells grown on coverslips were incubated with $T_{\lambda 600}$ or $T_{\lambda 600}$-loaded micelles for 5 or 60 minutes. Then, the cells were washed 3 times with PBS, fixed with 4% formaldehyde and mounted using Flouromount (Sigma-Aldrich). Images were acquired on a LV1200 CLSM (Olympus, Tokyo, Japan).

2.9. Flow cytometry

LNCaP cells were detached with TrypLE Express (Thermo Fisher). After centrifugation for 2 minutes at 1000g, cells were resuspended with $T_{\lambda 600}$, GM1- $T_{\lambda 600}$ or vehicles and incubated for 5 or 60 minutes at 37ºC. Cells were fixed with Cytofix (BD Biosciences Pharmingen, San Diego, CA), resuspended in filtrated PBS and analyzed using a FACSCanto II cytometer (Becton Dickinson, San Jose, CA).

2.10. Western blot

The procedure was performed as previously described [25]. Briefly, cells were lysed, sonicated and centrifuged for 30 minutes at 16,000g. Protein concentration was quantified using Bradford method. Samples were denatured, separated on 10% SDS–polyacrylamide gels and blotted onto Hybond-C membrane (Amersham Pharmacia, Buckinghamshire, UK). Membranes were incubated overnight at 4ºC with primary antibodies against pERK1/2

(1:1000, cell signaling, Danvers, MA), ERK1/2 (1:500, Santa Cruz Biotechnology, Santa Cruz, CA), pAkt (1:700, cell signaling), AR (1:500, Abcam, Cambridge, UK), ACTB (1:10000, Sigma-Aldrich) or PARP1 (1:100, Santa Cruz Biotechnology) washed and incubated with secondary antibodies conjugated to horseradish peroxidase (Jackson Immunoresearch Labs Inc., West Grove, PA) for 1 hour at room temperature. Membranes were revealed with luminol (Sigma-Aldrich) and emitted light was captured on hyperfilm (Amersham Pharmacia).

In order to obtain cytosolic and nuclear fractions, homogenates were first incubated with 1mM HEPES (pH 7,5), 60 mM KCl, 1 mM DTT, 0.045 v/v NP-40 and 1mM EDTA. Cells were scrapped and centrifuged for 10 minutes at 10,000g. The supernatant was then recovered as the cytoplasmic fraction while the pellet was resuspended in 20 mM Tris (pH 8), 420 mM NaCl, 60 mM KCl, 1 mM EDTA and 25% v/v glycerol and centrifuged for 10 minutes at 10,000g. This supernatant was recovered as the nuclear fraction.

2.11. RNA extraction, cDNA synthesis, and qPCR.

Total RNA was purified using the Direct-zol RNA miniprep kit (Zymo Research, Irvine, CA) accordingly to the manufacturer´s instructions. For reverse transcription, M-MLV Reverse transcriptase (Inbio Highway, Argentina) was used. The complementary DNA (cDNA) obtained was subjected to qPCR performed on an ABI Prism 7500 detection system (Thermo Fisher Scientific, Waltham, MA) using Power SYBR Green PCR Master Mix (Thermo Fisher Scientific), as previously reported [26]. The following human gene-specific primers were used: *PSA*: 5'-ACCAGAGGAGTTCTTGACCCCAAA (forward) and 5'-CCCCAGAATCACCCGAGCAG (reverse), *TMPRSS2*: 5'-CTGCTGGATTTCCGGGTG (forward) and 5'-TTCTGAGGTCTTCCCTTTCTCCT (reverse), *GADPH*: 5'-

CGCTCTCTGCTCCTCCTGTTC (forward) and 5'-TTGACTCCGACCTTCACCTTCC (reverse). Relative changes in gene expression were calculated using the $2^{-\Delta\Delta Ct}$ normalized against the housekeeping gene GAPDH. For each pair of primers, a dissociation plot resulted in a single peak, indicating that only one cDNA species was amplified. Amplification efficiency for each pair of primers was calculated using standard curves generated by serial dilutions of cDNA obtained from unstimulated cells. All amplification efficiencies ranged between 97% - 105%.

2.12. *In vivo* experiments

Male Albino Swiss mice of 3 months of age were castrated via the scrotal route. Six days after castration, animals received i.p. injections of testosterone in ethanol (0.1 mg/kg), GM1 (50 mg/kg)-T (0.1 mg/kg), or their vehicles (ethanol and GM1 respectively) every 12 hours for 3 days. Mice were anesthetized by isoflurane inhalation and sacrificed. Ventral prostates were surgically removed, photographed, weighed, and fixed using 4% formaldehyde for standard histological analysis.

2.13. Proliferation assay

Cells were incubated with 100 nM bromodeoxyuridine (BrdU) (Sigma-Aldrich) for 24 hours prior to fixation. Cells were subjected to antigen retrieval and DNA was digested by incubating with DNase (Zymo Research) for 40 minutes at 37ºC. Cell permeabilization was performed using 0.25% Triton X-100 (Sigma-Aldrich) and nonspecific immunoreactivity blocked with 5% BSA. Cells were then incubated overnight at 4ºC with an anti-BrdU antibody (1:200, BD Biosciences Pharmingen). Afterward, cells were washed and incubated with an Alexa 594 anti-rabbit antibody (1:1000, Jackson Immunoresearch Labs

Inc.) for 1 hour at room temperature. Incubation with 4',6-diamidino-2-phenylindole (DAPI) was used to stain cell nuclei. Images were acquired on an epifluorescent microscope (Zeiss, Oberkochen, Germany). A total of 1,000 cells were counted in randomly chosen fields of each glass slide to establish the percentage of BrdU positive cells. Three slides were analyzed for each group.

Alternatively, proliferation of HPSC was analyzed by immunostaining using an anti-Ki67 antibody (1:30, BD Biosciences Pharmingen). Cells were then incubated for 1 hour with an anti-mouse antibody conjugated to biotin (1:100, Amersham Pharmacia) and later for 30 minutes with avidin–peroxidase complex (Vector, Burlingame, CA). The immunoreactivity for Ki67 was visualized with 3,3-diaminobenzidine tetrahydrochloride (DAB) as chromogen (Sigma-Aldrich).

2.14. Statistical Analysis

All experiments were replicated at least three times with independent cell cultures. Data from three or more independent groups were analyzed using ANOVA-Tukey. Differences between two means were considered as statistically significant when $p<0.05$. Statistical testing was performed using the software GraphPad Prism version 8.0.2 (La Jolla, CA).

3. Results

3.1 Characterization of testosterone-loaded GM1 micelles

The formulation of GM1 (Fig. 1a) micelles with hydrophobic drugs has been reported to increase micellar stability [18,19]. Furthermore, while other nanoparticles have shown to change size when interacting with different molecules, GM1 micelles could maintain their size, which is a critical parameter for *in vivo* delivery [19]. To determine the ideal molar ratio of testosterone (Fig. 1a) to GM1, different concentrations of testosterone were loaded into micelles, samples were centrifuged at 20,000g for 30 minutes and the insoluble testosterone was measured by ECLIA. Accordingly, a molar ratio of testosterone to GM1 of 1:100 allowed all testosterone to be loaded into the micelles (data not shown), and it was used for all further experiments.

The size and rounded morphology of GM1 and GM1-T micelles were determined by TEM (Fig. 1b) and confirmed by DLS (Fig. 1c). The diameter of both empty and loaded micelles was of approximately 5-11 nm, showing no changes after testosterone loading. To analyze the effects of pH on GM1-T micelle stability, GM1-T micelles were diluted in different acidic or alkaline buffers. We observed that in acidic medium (pH 3 and pH 5) micelles tend to aggregate and increase their size, while in neutral (pH 7) or alkaline (pH 10) media, micelle size was less variable (Supplementary Fig. 1).

As previously demonstrated, size exclusion liquid chromatography revealed that GM1 molecules are present in both, monomeric and micellar (aggregate) states [19]. When these molecules were mixed with hydrophobic molecules of testosterone in GM1-T, the balance was completely modified towards the micellar state, with free GM1 molecules being undetected (Fig. 1d). This result indicates that testosterone loading increases micellar stability as it had been shown for other hydrophobic drugs [19].

To analyze if testosterone is retained in GM1 micelles, a dialysis assay was performed to elute free testosterone by using 12kD-cut-off membranes, with the remaining solution being tested by ECLIA. We observed that testosterone previously loaded into GM1 micelles was unable to diffuse through the dialysis membrane, indicating that testosterone was completely retained in the micelles. As a control, when free testosterone was dialyzed using the same type of membranes, almost all of the testosterone molecules were lost after 2 hours of dialysis (Fig. 1e). To confirm this finding, we used $T_{\lambda 600}$ which emits fluorescence with a maximum intensity at 620nm. Retention of $T_{\lambda 600}$ in GM1 micelles was analyzed after 1 and 2 hours of dialysis using a Glomax Discovery Microplate Reader. As shown for testosterone, GM1 micelles were also able to preserve $T_{\lambda 600}$ (Fig. 1f).

In order to determine the optimal working conditions *in vitro*, we next determined effects of GM1 on cell viability. LNCaP and rPSC were stimulated with different doses of GM1 for 24 hours. Viability of both cell types was significantly reduced after stimuli with GM1 at concentrations above 50 μg/ml (Fig. 2). Considering this result and the optimal testosterone to GM1 molar ratio determined before, we decided to use $1x10^{-6}$M (1.6 μg/ml) of GM1 in all further experiments.

3.2 Testosterone loaded- GM1 micelles deliver testosterone within the cell

In order to assess if GM1-T can induce genomic androgen signaling, we first studied whether GM1-T micelles can deliver testosterone inside the cell. Taking advantage of $T_{\lambda 600}$ (Fig. 3a) for cellular tracking at 620nm, LNCaP cells were incubated with $T_{\lambda 600}$ or GM1-$T_{\lambda 600}$ for 5 or 60 minutes and analyzed by confocal microscopy. We observed that GM1 micelles are able to effectively deliver testosterone inside the cell at the same rate than that of free testosterone. In both cases, $T_{\lambda 600}$ was observed within the cell as soon as 5 minutes after

treatment, with its signal being increased in a time-dependent manner (Fig. 3b). When the incubation was performed after a 2 hour dialysis of $T_{\lambda 600}$ or GM1-$T_{\lambda 600}$, the fluorescent signal was observed only when $T_{\lambda 600}$ had been loaded into GM1 micelles. Then, we corroborated these results by flow cytometry, showing that the fluorescence intensity increased equally in cells stimulated with $T_{\lambda 600}$ or GM1-$T_{\lambda 600}$, as compared to their controls (Fig. 3c). These findings demonstrate the ability of GM1 to retain testosterone, which is in agreement with the characterization described in result section 3.1, and to deliver testosterone inside the cell.

3.3 Genomic androgen signaling is induced after stimulation with testosterone loaded-GM1 micelles

Genomic androgen signaling requires testosterone binding to the AR in the cytoplasm and later translocation to the nucleus, where the hormone-ligand complex interacts with specific AREs in the gene promoter regions of the DNA [27]. Genes such as *AR*, *PSA,* and *TMPRSS2* are highly regulated by androgens through ARE-containing sequences, and thus they are good reporters for genomic androgen signaling [28,29]. To determine AR genomic activity in cells stimulated with GM1-T, we first analyzed AR expression in the tumor cell line LNCaP and in normal rPSC. We showed that AR increases in response to both testosterone and GM1-T in a concentration-dependent manner (Fig. 4a and b). AR expression was highest at 10^{-8}-10^{-7}M of testosterone and GM1-T in both cell types, and thus further experiments were carried out with a concentration of 10^{-8}M, since this is closer to the physiological concentration in blood. Then, we analyzed the expression of mRNA for *PSA* and *TMPRSS2* by qPCR in LNCaP cells after treatment with testosterone or GM1-T for 8 hours; a significant increase for both ARE-regulated genes was shown after both stimuli (Fig. 4c and 4d). In addition, we analyzed nuclear translocation of the AR, a key aspect of genomic

androgen signaling. We demonstrated that the stimulation of LNCaP cells with GM1-T induced significant translocation of the AR to the nucleus, similarly to that induced by testosterone (Fig. 4e).

Androgens control male characteristics including prostatic size and function by activating specific ARE-containing genes at the cellular level [30]. Hence, castration leads to a rapid and extensive atrophy in the whole male tract, with testosterone administration being able to restore male characteristics [31]. To determine if GM1-T maintains this behavior, male mice were castrated and then treated with i.p. injections of testosterone, GM1-T, or their vehicles. As expected, testosterone at a physiological dose, increased prostate complex size (Fig. 5a) and weight (Fig. 5b) of castrated mice, being similar to those of sham-operated animals. Testosterone also recovered normal histology and function in the gland, including the height of columnar epithelial cells and abundant secretion in the acinar lumen (Fig. 5c). Likewise, GM1-T-injected-mice were able to recover ventral prostate parameters similarly to those injected with testosterone (Fig. 5a-c), indicating that GM1-T exerts strong genomic effects *in vivo*. In contrast, vehicle-treated mice showed atrophic prostates with lack of observable secretion (Fig. 5a-c). To determine if GM1-T is capable of inducing cell proliferation, necessary for restoration of prostate size, we analyzed incorporation of BrdU *in vitro* using rPSC. Stimuli with testosterone-loaded micelles for 24 hours induced an increase in cell proliferation to similar levels of those promoted by testosterone (Fig. 5d). These results were corroborated in HPSC, where GM1-T showed a concentration-dependent effect on cell proliferation (Supplementary Fig. 2).

3.4 Delivery of testosterone through GM1 micelles bypasses MIAS

As GM1-T micelles have proved to be very efficient in the induction of genomic androgen signaling, we then addressed the activation of MIAS after GM1-T treatment. MIAS is best characterized by the activation of ionic channels, Ca^{2+} mobilization, and rapid downstream pathways including MAPK, PI3K/Akt, PKA, and PKC, leading to different transcriptional programs [32,33]. To analyze the effects of GM1-T on MIAS, phosphorylation of ERK1/2 and Akt was analyzed by western blots in homogenates of rPSC and LNCaP cells treated with testosterone, GM1-T, T-BSA or their vehicles for 30 or 60 minutes. We observed that while testosterone and T-BSA stimulated phosphorylation of ERK1/2 and Akt, GM1-T was unable to reproduce these effects, suggesting that GM1-T does not activate MIAS (Fig. 6a and b).

We have previously reported that intracellular AR activation could result in the induction of both pro- and anti-proliferative factors in prostatic stromal cells, with a highly regulated balance favoring homeostatic cell survival and proliferation [7]. On the other hand, MIAS leads to a higher proliferation rate, which might promote and maintain the uncontrolled pathogenic hyperproliferative status of BPH [7]. To compare the effects of the genomic androgen signaling to those of MIAS on cell proliferation, rPSC were stimulated for 24 hours with GM1-T micelles or T-BSA respectively, and cell proliferation was determined by BrdU incorporation; as expected a higher proliferation was observed in cells stimulated with T-BSA (Fig. 6c). Increased cell proliferation by specific stimulation of MIAS was also observed in HPCS (Supplementary Fig. 3). These results evidence the critical role of genomic androgen signaling in the induction of a controlled proliferative status in the prostate gland, as previously suggested [7].

4. Discussion

In the present article, we report a novel strategy to activate genomic androgen signaling pathways while bypassing pathogenic MIAS. This has been achieved by the use of a micellar structure formed by GM1 molecules, which is able to encapsulate testosterone protecting it from being recognized by plasma membrane receptors. The induction of genomic signaling was demonstrated by the specific expression of ARE-regulated genes and AR nuclear translocation, whereas the absence of MIAS was evaluated by analyzing the rapid activation of transduction pathways. In addition, we show that the intracellular delivery of testosterone by GM1 micelles promotes homeostatic cell proliferation of rat normal prostatic stromal cells as well as of stromal cells derived from patients with BPH, contrasting with the significantly higher proliferation induced by MIAS.

Drug delivery through nanoparticles has considerable benefits, including enhanced solubility, greater stability, lower clearance, minimal toxicity, decreased immunogenicity, controlled release, and site-specific delivery [34]. Our goal in this study was to use the advantages of nanoparticle intracellular drug delivery to specifically activate nuclear-induced genomic androgen signaling. Furthermore, GM1 micellar nanoparticles have shown additional benefits such as self-assembly [19], escape from the reticuloendothelial system [35], ability to passively reach tumors due to the enhanced permeability and retention effect [19], and a very low CMC (10^{-10}-10^{-8}M) that allows for higher dilutions than other types of micelles.

In aqueous solutions and at concentrations above the CMC, GM1 molecules show a dynamic balance between free molecules and micellar aggregates [36]. It has been reported that while GM1 monomers enter the plasma membrane, GM1 micelles bind to the cell surface and enter the cell through endocytosis [17]. In this study we show that the addition of

testosterone to GM1 micelles has no effects on particle size but modifies the dynamic balance stabilizing GM1 in their micellar state. The same effect was observed when GM1 interacted with hydrophobic drugs such as paclitaxel and docetaxel [19]. Although we do not know the exact location of testosterone in this micellar system, studies using other hydrophobic drugs suggest that they would locate at the internal hydrophobic core [18]. Interestingly, we demonstrate that the interaction of GM1 with testosterone impedes the simple diffusion of the steroid through a selective membrane. Furthermore, to corroborate whether GM1 is able to deliver testosterone inside the cell, in this article we used a fluorescent-modified testosterone and observed that intracellular delivery of testosterone through GM1 micelles is effective, occurring as soon as 5 minutes after treatment.

Cellular responses to androgens depend, among other aspects, on the type of receptor involved and on its subcellular localization [7,37]. According to this, androgen signaling can be divided into: genomic, when the AR located at the cytosol binds its ligand and migrates to the nucleus in order to act as a ligand-activated transcription factor [38]; or MIAS, when androgens interact with plasma membrane receptors such as GPRC6A [39], TRPM8 [40], ZIP9 [41], OXER1 [42], or cell surface-localized AR [5,43]. Several strategies aiming to preferentially stimulate a specific set of receptors have been developed in order to study the different signaling mechanisms of androgens. Approaches like testosterone-BSA conjugates succeeded to modulate cell proliferation of prostate epithelial and stromal cells through specific stimulation of MIAS [44,45,7]. In addition, inhibition of MIAS through S1 peptide, corresponding to the proline-rich domain of AR, or peptidomimetics has shown the contribution of MIAS to spermatogenesis [46]. On the contrary, agonists of the genomic signaling pathways have not been developed, leaving many actions of the cytosolic AR unclarified. Noteworthy, the use of estrogen-loaded liposomes as a tool for selective

activation of genomic pathways induced by the estrogen receptor has been recently reported [47]. In agreement with these results, genomic signaling and MIAS could be perfectly dissected and it points nanocarriers as an excellent alternative for hormone research and therapeutics. Our results here demonstrate that testosterone loaded into GM1 micelles induces genomic signaling responses such as activation of ARE-regulated genes and prostatic size recovery in castrated rats, while prevents the activation of the MIAS mechanisms.

Androgen signaling induces cell proliferation which contributes to the progression of BPH and PCa [1,2]. Determining the contribution of each androgen signaling pathway to cell proliferation has been a challenging task mainly due to the lack of strong tools for pathway-specific activation. It is known that MIAS activates pathogenic proliferative transduction pathways such as MAPK through EGFR phosphorylation [48] and PI3K/Akt pathways [49]. In addition, up-regulation of IGF-1R has been associated with non-genomic signaling and could also lead to pathogenic proliferation [50,51]. On the other hand, genomic androgen signaling has also shown to induce proliferative pathways such as the activation of genes involved in DNA replication [52-54] and growth factors [55]. Furthermore, other pro-proliferative ARE-regulated genes have been observed in prostatic stromal cells [56]. Higher levels of proliferation in cells stimulated with MIAS agonists can be explain by the lower expression of anti-proliferative genes [7]. Here, we show that although testosterone-loaded GM1 micelles induce cell proliferation, it occurs at lower levels than those induced by MIAS. Uncontrolled stromal cell proliferation is a crucial aspect in the development of mixed and of stromal nodules of BPH [57]. Here, we propose that by selectively activating genomic androgen signaling using GM1-T, we can promote homeostatic proliferation avoiding the negative effects of MIAS and/or androgen deprivation.

Our *in vivo* results show that GM1-T is able to recover normal prostate size and histology after ip administration. Although we have not addressed the mechanisms by which GM1-T micelles can reach the prostate, it has been described that uncharged particles smaller than 10nm can enter directly into the blood stream, with this being a possible route for GM1-T micelles. An alternative choice is that these nanoparticles enter the systemic circulation through absorption by lymphatic ducts in the peritoneum [58]. While direct absorption through blood vessels is a much faster mechanism, larger molecules may pass through the peritoneal stomata into the lymph [59,60], if this were the case for GM1-T, their relative small size (<50nm) would allow them to avoid being trapped in the lymph nodes and eventually reach blood circulation [58]. The *in vivo* findings presented in this article allow us to conclude that, after being encapsulated by GM1, testosterone can still maintain full androgenic activity, yet the complex mechanisms that lead to the in vivo delivery of GM1-T are still unclear and needed to be determined

Depending on their subcellular localization, testosterone receptors can regulate a wide set of very distinct cellular mechanisms. Thus, novel compounds targeting specific subcellular pools of receptors could favor desired effects while avoiding many unwanted side-effects of testosterone when an androgen replacement therapy is used in aging hypogonadic men. Novel and more sophisticated nanodelivery systems are being constantly developed. Strategies for organ-specific delivery and subcellular targeting have already been generated, granting important benefits by reducing secondary side-effects [61,62]. In addition, vehicles targeted to specific subcellular compartments are interesting tools for delivering androgens away from the cell surface and MIAS. We here report specific activation of the genomic signaling of testosterone by using a simple and stable GM1 micelle.

This represents a first step in the future development of a more precise subcellular delivery of androgens through nanoparticles in order to favor specific-receptor activation.

Abbreviations

AR: Androgen receptor; MIAS: Membrane-initiated androgen signaling; GM1: Monosialoganglioside; BPH: Benign prostatic hyperplasia; CMC: Critical micellar concentration; GM1-T: Testosterone-loaded GM1 micelle; $T_{\lambda 600}$: Fluorescent testosterone; rPSC: Rat prostate stromal cells; HPSC: Human prostatic stromal cells from patients with BPH; T-BSA: Testosterone-bovine serum albumin conjugate; ARE: Androgen response elements; PSA: Prostate-specific antigen; TMPRSS2: Transmembrane protease serine 2.

Acknowledgments

The authors wish to acknowledge Carolina Leimgruber (INICSA-CONICET) for the excellent technical assistance in TEM processing, Elba Vazquez (IQUIBICEN-CONICET) and Emiliano Ortiz (IQUIBICEN-CONICET) for providing the LNCaP cell line, Ricardo Fretes (INICSA-CONICET) for kindly granting access to all of his laboratory equipment, and Dr. Manuel Lopez Seoane (Urology Department, Sanatorio Allende, Córdoba, Argentina) for participation in everything concerning human samples acquisition.

Funding

This work was supported by Consejo Nacional de Investigaciones Científicas y Técnicas (CONICET to C.A.M. and A.A.Q), Secretaría de Ciencia y Tecnología, Universidad Nacional de Córdoba (SECyT-UNC to C.A.M. and A.A.Q), and Agencia Nacional de

Promoción Científica y Tecnológica–Ministerio de Ciencia y Tecnología (FONCyT PICT to A.A.Q. and C.A.M.).

References

1. Wong YN, Ferraldeschi R, Attard G, de Bono J (2014) Evolution of androgen receptor targeted therapy for advanced prostate cancer. Nature reviews Clinical oncology 11 (6):365-376. doi:10.1038/nrclinonc.2014.72

2. Chughtai B, Forde JC, Thomas DD, Laor L, Hossack T, Woo HH, Te AE, Kaplan SA (2016) Benign prostatic hyperplasia. Nature reviews Disease primers 2:16031. doi:10.1038/nrdp.2016.31

3. Cunha GR (2008) Mesenchymal-epithelial interactions: past, present, and future. Differentiation; research in biological diversity 76 (6):578-586. doi:10.1111/j.1432-0436.2008.00290.x

4. Matsumoto T, Sakari M, Okada M, Yokoyama A, Takahashi S, Kouzmenko A, Kato S (2013) The androgen receptor in health and disease. Annual review of physiology 75:201-224. doi:10.1146/annurev-physiol-030212-183656

5. Levin ER, Hammes SR (2016) Nuclear receptors outside the nucleus: extranuclear signalling by steroid receptors. Nature reviews Molecular cell biology 17 (12):783-797. doi:10.1038/nrm.2016.122

6. Leung JK, Sadar MD (2017) Non-Genomic Actions of the Androgen Receptor in Prostate Cancer. Frontiers in endocrinology 8:2. doi:10.3389/fendo.2017.00002

7. Peinetti N, Scalerandi MV, Cuello Rubio MM, Leimgruber C, Nicola JP, Torres AI, Quintar AA, Maldonado CA (2018) The Response of Prostate Smooth Muscle Cells to Testosterone Is Determined by the Subcellular Distribution of the Androgen Receptor. Endocrinology 159 (2):945-956. doi:10.1210/en.2017-00718

8. Vignozzi L, Cellai I, Santi R, Lombardelli L, Morelli A, Comeglio P, Filippi S, Logiodice F, Carini M, Nesi G, Gacci M, Piccinni MP, Adorini L, Maggi M (2012) Antiinflammatory effect of androgen receptor activation in human benign prostatic hyperplasia cells. The Journal of endocrinology 214 (1):31-43. doi:10.1530/JOE-12-0142

9. Quintar AA, Leimgruber C, Pessah OA, Doll A, Maldonado CA (2012) Androgen depletion augments antibacterial prostate host defences in rats. Int J Androl 35 (6):845-859

10. Scalerandi MV, Peinetti N, Cuello Rubio MM, Nicola JP, Leimgruber C, Menezes GB, Maldonado CA, Quintar AA (2018) Inefficient N2-like Neutrophils Are Promoted by Androgens During Infection. Frontiers in Immunology

11. Kampa M, Kogia C, Theodoropoulos PA, Anezinis P, Charalampopoulos I, Papakonstanti EA, Stathopoulos EN, Hatzoglou A, Stournaras C, Gravanis A, Castanas E (2006) Activation of membrane androgen receptors potentiates the antiproliferative effects of paclitaxel on human prostate cancer cells. Molecular cancer therapeutics 5 (5):1342-1351. doi:10.1158/1535-7163.MCT-05-0527

12. Navarro G, Xu W, Jacobson DA, Wicksteed B, Allard C, Zhang G, De Gendt K, Kim SH, Wu H, Zhang H, Verhoeven G, Katzenellenbogen JA, Mauvais-Jarvis F (2016) Extranuclear Actions of the Androgen Receptor Enhance Glucose-Stimulated Insulin Secretion in the Male. Cell metabolism 23 (5):837-851. doi:10.1016/j.cmet.2016.03.015

13. Caracciolo G (2015) Liposome-protein corona in a physiological environment: challenges and opportunities for targeted delivery of nanomedicines. Nanomedicine : nanotechnology, biology, and medicine 11 (3):543-557. doi:10.1016/j.nano.2014.11.003

14. Boca S, Gulei D, Zimta AA, Onaciu A, Magdo L, Tigu AB, Ionescu C, Irimie A, Buiga R, Berindan-Neagoe I (2020) Nanoscale delivery systems for microRNAs in cancer therapy. Cellular and molecular life sciences : CMLS 77 (6):1059-1086. doi:10.1007/s00018-019-03317-9

15. Iversen TG, Skotland T, Sandvig K (2011) Endocytosis and intracellular transport of nanoparticles: present knowledge and need for future studies. Nano today 6 (2):176-185

16. Hillaireau H, Couvreur P (2009) Nanocarriers' entry into the cell: relevance to drug delivery. Cellular and molecular life sciences : CMLS 66 (17):2873-2896. doi:10.1007/s00018-009-0053-z

17. Aureli M, Mauri L, Ciampa MG, Prinetti A, Toffano G, Secchieri C, Sonnino S (2016) GM1 Ganglioside: Past Studies and Future Potential. Molecular neurobiology 53 (3):1824-1842. doi:10.1007/s12035-015-9136-z

18. Leonhard V, Alasino RV, Bianco ID, Garro AG, Heredia V, Beltramo DM (2015) Biochemical characterization of the interactions between doxorubicin and lipidic GM1 micelles with or without paclitaxel loading. International journal of nanomedicine 10:3377-3387. doi:10.2147/IJN.S77153

19. Leonhard V, Alasino RV, Bianco ID, Garro AG, Heredia V, Beltramo DM (2012) Self-assembled micelles of monosialogangliosides as nanodelivery vehicles for taxanes. Journal of controlled release : official journal of the Controlled Release Society 162 (3):619-627. doi:10.1016/j.jconrel.2012.07.031

20. Leonhard V, Alasino RV, Bianco ID, Garro AG, Heredia V, Beltramo DM (2015) Biochemical characterization of GM1 micelles-Amphotericin B interaction. Current drug delivery 12 (4):406-414

21. Eechaute W, Demeester G, Leusen I (1970) A sensitive sulfuric acid-ethanol induced fluorescence reaction for testosterone and androstenedione. Steroids 16 (3):277-287. doi:10.1016/s0039-128x(70)80113-1

22. Takagi H, Miura T, Kimura M (1982) Further Studies on the Mechanism of the Color and Fluorescence Reaction of Testosterone with Sulfuric Acid. Chemical & Pharmaceutical Bulletin 30 (10):3493-3499

23. Leimgruber C, Quintar AA, Peinetti N, Scalerandi MV, Nicola JP, Miano JM, Maldonado CA (2017) Testosterone Rescues the De-Differentiation of Smooth Muscle Cells Through Serum Response Factor/Myocardin. Journal of cellular physiology 232 (10):2806-2817. doi:10.1002/jcp.25679

24. Leimgruber C, Quintar AA, Sosa LD, García LN, Figueredo M, Maldonado CA (2011) Dedifferentiation of prostate smooth muscle cells in response to bacterial LPS. Prostate 71 (10):1097-1107

25. Sosa LDV, Petiti JP, Picech F, Chumpen S, Nicola JP, Perez P, De Paul A, Valdez-Taubas J, Gutierrez S, Torres AI (2019) The ERalpha membrane pool modulates the proliferation of pituitary tumours. The Journal of endocrinology 240 (2):229-241. doi:10.1530/JOE-18-0418

26. Peyret V, Nazar M, Martin M, Quintar AA, Fernandez EA, Geysels RC, Fuziwara CS, Montesinos MM, Maldonado CA, Santisteban P, Kimura ET, Pellizas CG, Nicola JP, Masini-Repiso AM (2018) Functional Toll-like Receptor 4 Overexpression in Papillary Thyroid Cancer by MAPK/ERK-Induced ETS1 Transcriptional Activity. Molecular cancer research : MCR 16 (5):833-845. doi:10.1158/1541-7786.MCR-17-0433

27. Zamagni A, Cortesi M, Zanoni M, Tesei A (2019) Non-nuclear AR Signaling in Prostate Cancer. Frontiers in chemistry 7:651. doi:10.3389/fchem.2019.00651

28. Cleutjens KB, van der Korput HA, van Eekelen CC, van Rooij HC, Faber PW, Trapman J (1997) An androgen response element in a far upstream enhancer region is essential for high, androgen-regulated activity of the prostate-specific antigen promoter. Molecular endocrinology 11 (2):148-161. doi:10.1210/mend.11.2.9883

29. Grad JM, Dai JL, Wu S, Burnstein KL (1999) Multiple androgen response elements and a Myc consensus site in the androgen receptor (AR) coding region are involved in androgen-mediated up-regulation of AR messenger RNA. Molecular endocrinology 13 (11):1896-1911. doi:10.1210/mend.13.11.0369

30. Notini AJ, Davey RA, McManus JF, Bate KL, Zajac JD (2005) Genomic actions of the androgen receptor are required for normal male sexual differentiation in a mouse model. Journal of molecular endocrinology 35 (3):547-555. doi:10.1677/jme.1.01884

31. Silva JAF, Bruni-Cardoso A, Augusto TM, Damas-Souza DM, Barbosa GO, Felisbino SL, Stach-Machado DR, Carvalho HF (2018) Macrophage roles in the clearance of apoptotic cells and control of inflammation in the prostate gland after castration. Prostate 78 (2):95-103. doi:10.1002/pros.23449

32. Bennett NC, Gardiner RA, Hooper JD, Johnson DW, Gobe GC (2010) Molecular cell biology of androgen receptor signalling. The international journal of biochemistry & cell biology 42 (6):813-827. doi:10.1016/j.biocel.2009.11.013

33. Zarif JC, Miranti CK (2016) The importance of non-nuclear AR signaling in prostate cancer progression and therapeutic resistance. Cellular signalling 28 (5):348-356. doi:10.1016/j.cellsig.2016.01.013

34. Patra JK, Das G, Fraceto LF, Campos EVR, Rodriguez-Torres MDP, Acosta-Torres LS, Diaz-Torres LA, Grillo R, Swamy MK, Sharma S, Habtemariam S, Shin HS (2018) Nano based drug delivery systems: recent developments and future prospects. Journal of nanobiotechnology 16 (1):71. doi:10.1186/s12951-018-0392-8

35. Heredia V, Alasino RV, Leonhard V, Garro AG, Maggio B, Beltramo DM (2016) Sialoganglioside Micelles for Enhanced Paclitaxel Solubility: In Vitro Characterization. Journal of pharmaceutical sciences 105 (1):268-275. doi:10.1016/j.xphs.2015.10.029

36. Saqr HE, Pearl DK, Yates AJ (1993) A review and predictive models of ganglioside uptake by biological membranes. Journal of neurochemistry 61 (2):395-411. doi:10.1111/j.1471-4159.1993.tb02140.x

37. Lutz LB, Jamnongjit M, Yang WH, Jahani D, Gill A, Hammes SR (2003) Selective modulation of genomic and nongenomic androgen responses by androgen receptor ligands. Molecular endocrinology 17 (6):1106-1116. doi:10.1210/me.2003-0032

38. Liao RS, Ma S, Miao L, Li R, Yin Y, Raj GV (2013) Androgen receptor-mediated non-genomic regulation of prostate cancer cell proliferation. Translational andrology and urology 2 (3):187-196. doi:10.3978/j.issn.2223-4683.2013.09.07

39. Pi M, Parrill AL, Quarles LD (2010) GPRC6A mediates the non-genomic effects of steroids. The Journal of biological chemistry 285 (51):39953-39964. doi:10.1074/jbc.M110.158063

40. Asuthkar S, Demirkhanyan L, Sun X, Elustondo PA, Krishnan V, Baskaran P, Velpula KK, Thyagarajan B, Pavlov EV, Zakharian E (2015) The TRPM8 protein is a testosterone receptor: II. Functional evidence for an ionotropic effect of testosterone on TRPM8. The Journal of biological chemistry 290 (5):2670-2688. doi:10.1074/jbc.M114.610873

41. Thomas P, Pang Y, Dong J, Berg AH (2014) Identification and characterization of membrane androgen receptors in the ZIP9 zinc transporter subfamily: II. Role of human ZIP9 in testosterone-induced prostate and breast cancer cell apoptosis. Endocrinology 155 (11):4250-4265. doi:10.1210/en.2014-1201

42. Kalyvianaki K, Gebhart V, Peroulis N, Panagiotopoulou C, Kiagiadaki F, Pediaditakis I, Aivaliotis M, Moustou E, Tzardi M, Notas G, Castanas E, Kampa M (2017) Antagonizing effects of membrane-acting androgens on the eicosanoid receptor OXER1 in prostate cancer. Scientific reports 7:44418. doi:10.1038/srep44418

43. Li J, Fu X, Cao S, Li J, Xing S, Li D, Dong Y, Cardin D, Park HW, Mauvais-Jarvis F, Zhang H (2018) Membrane-associated androgen receptor (AR) potentiates its transcriptional activities by activating heat shock protein 27 (HSP27). The Journal of biological chemistry 293 (33):12719-12729. doi:10.1074/jbc.RA118.003075

44. Pedram A, Razandi M, Sainson RC, Kim JK, Hughes CC, Levin ER (2007) A conserved mechanism for steroid receptor translocation to the plasma membrane. The Journal of biological chemistry 282 (31):22278-22288. doi:10.1074/jbc.M611877200

45. Papadopoulou N, Charalampopoulos I, Anagnostopoulou V, Konstantinidis G, Foller M, Gravanis A, Alevizopoulos K, Lang F, Stournaras C (2008) Membrane androgen receptor activation triggers down-regulation of PI-3K/Akt/NF-kappaB activity and induces apoptotic responses via Bad, FasL and caspase-3 in DU145 prostate cancer cells. Molecular cancer 7:88. doi:10.1186/1476-4598-7-88

46. Toocheck C, Clister T, Shupe J, Crum C, Ravindranathan P, Lee TK, Ahn JM, Raj GV, Sukhwani M, Orwig KE, Walker WH (2016) Mouse Spermatogenesis Requires Classical and Nonclassical Testosterone Signaling. Biol Reprod 94 (1):11. doi:10.1095/biolreprod.115.132068

47. Gallez A, Palazzo C, Blacher S, Tskitishvili E, Noel A, Foidart JM, Evrard B, Pequeux C, Piel G (2020) Liposomes and drug-in-cyclodextrin-in-liposomes formulations encapsulating 17beta-estradiol: An innovative drug delivery system that prevents the activation of the membrane-initiated steroid signaling (MISS) of estrogen receptor alpha. International journal of pharmaceutics 573:118861. doi:10.1016/j.ijpharm.2019.118861

48. Sen A, O'Malley K, Wang Z, Raj GV, Defranco DB, Hammes SR (2010) Paxillin regulates androgen- and epidermal growth factor-induced MAPK signaling and cell proliferation in prostate cancer cells. The Journal of biological chemistry 285 (37):28787-28795. doi:10.1074/jbc.M110.134064

49. Castoria G, Auricchio F, Migliaccio A (2017) Extranuclear partners of androgen receptor: at the crossroads of proliferation, migration, and neuritogenesis. FASEB journal : official publication of the Federation of American Societies for Experimental Biology 31 (4):1289-1300. doi:10.1096/fj.201601047R

50. Malaguarnera R, Sacco A, Morcavallo A, Squatrito S, Migliaccio A, Morrione A, Maggiolini M, Belfiore A (2014) Metformin inhibits androgen-induced IGF-IR up-regulation in prostate cancer cells by disrupting membrane-initiated androgen signaling. Endocrinology 155 (4):1207-1221. doi:10.1210/en.2013-1925

51. Kasprzak A, Kwasniewski W, Adamek A, Gozdzicka-Jozefiak A (2017) Insulin-like growth factor (IGF) axis in cancerogenesis. Mutation research Reviews in mutation research 772:78-104. doi:10.1016/j.mrrev.2016.08.007

52. Jin F, Fondell JD (2009) A novel androgen receptor-binding element modulates Cdc6 transcription in prostate cancer cells during cell-cycle progression. Nucleic acids research 37 (14):4826-4838. doi:10.1093/nar/gkp510

53. Cao R, Ke M, Wu Q, Tian Q, Liu L, Dai Z, Lu S, Liu P (2019) AZGP1 is androgen responsive and involved in AR-induced prostate cancer cell proliferation and metastasis. Journal of cellular physiology 234 (10):17444-17458. doi:10.1002/jcp.28366

54. Bolton EC, So AY, Chaivorapol C, Haqq CM, Li H, Yamamoto KR (2007) Cell- and gene-specific regulation of primary target genes by the androgen receptor. Genes & development 21 (16):2005-2017. doi:10.1101/gad.1564207

55. Lamont KR, Tindall DJ (2010) Androgen regulation of gene expression. Advances in cancer research 107:137-162. doi:10.1016/S0065-230X(10)07005-3

56. Nash C, Boufaied N, Mills IG, Franco OE, Hayward SW, Thomson AA (2018) Genome-wide analysis of AR binding and comparison with transcript expression in primary human fetal prostate fibroblasts and cancer associated fibroblasts. Molecular and cellular endocrinology 471:1-14. doi:10.1016/j.mce.2017.05.006

57. Strand DW, Costa DN, Francis F, Ricke WA, Roehrborn CG (2017) Targeting phenotypic heterogeneity in benign prostatic hyperplasia. Differentiation; research in biological diversity 96:49-61. doi:10.1016/j.diff.2017.07.005

58. Au JL, Lu Z, Wientjes MG (2015) Versatility of Particulate Carriers: Development of Pharmacodynamically Optimized Drug-Loaded Microparticles for Treatment of Peritoneal Cancer. The AAPS journal 17 (5):1065-1079. doi:10.1208/s12248-015-9785-x

59. Mirahmadi N, Babaei MH, Vali AM, Dadashzadeh S (2010) Effect of liposome size on peritoneal retention and organ distribution after intraperitoneal injection in mice. International journal of pharmaceutics 383 (1-2):7-13. doi:10.1016/j.ijpharm.2009.08.034

60. Sarfarazi A, Lee G, Mirjalili SA, Phillips ARJ, Windsor JA, Trevaskis NL (2019) Therapeutic delivery to the peritoneal lymphatics: Current understanding, potential treatment benefits and future prospects. International journal of pharmaceutics 567:118456. doi:10.1016/j.ijpharm.2019.118456

61. Nag OK, Delehanty JB (2019) Active Cellular and Subcellular Targeting of Nanoparticles for Drug Delivery. Pharmaceutics 11 (10). doi:10.3390/pharmaceutics11100543

62. Arranja AG, Pathak V, Lammers T, Shi Y (2017) Tumor-targeted nanomedicines for cancer theranostics. Pharmacological research 115:87-95. doi:10.1016/j.phrs.2016.11.014

Figure Legends

Fig. 1: Characterization of testosterone-loaded GM1 micelles

a. Molecular structure of testosterone and of GM1, based on ref. [20]. **b.** Representative TEM images exhibiting empty (GM1) or testosterone-loaded GM1 micelles (GM1-T), negatively stained with phosphotungstic acid and observed at 167,000x. Scale bar = 100 nm. Histograms show the frequency of micellar size in each case, assessed in TEM pictures. **c.** Size of GM1 (green) or GM1-T (blue) micelles determined by DLS, denoting an individual peak around 10 nm of micellar diameter for both types of micelle. **d.** Size exclusion chromatography of empty GM1 micelles (green) showing two discrete peaks, belonging to the micellar (left) and the monomeric (right) forms of GM1. GM1-T micelles (blue) display only one peak corresponding to micellar aggregates, indicating that adding testosterone stabilizes the micellar structure of GM1. **e.** Concentration of testosterone in a solution of GM1-T, detected by ECLIA, demonstrating the retention of the hormone after 2 hours dialysis compared to the loss of free testosterone (T) in the same period (*p<0.05 vs. T input, n=3, ANOVA-Tukey). **f.** Concentration of $T_{\lambda 600}$ detected by fluorescence emission after 1 or 2 hours of dialysis of $T_{\lambda 600}$ or GM1-$T_{\lambda 600}$ solutions, corroborating the ECLIA data in **e** (*p<0.05 vs. $T_{\lambda 600}$ input, n=3, ANOVA-Tukey)

Fig. 2: Effects of GM1 on cell viability

Viability of LNCaP (**a**) and rPSC (**b**) after stimulation with 0.005-500 µg/ml GM1 for 24 hours. Cells were counted with Neubauer chamber after staining with trypan Blue to discard dead cells

Fig. 3: Cellular internalization of testosterone loaded into GM1 micelles

a. Molecular structure of $T_{\lambda 600}$, from ref. [22] **b.** Confocal images of LNCaP cells incubated with $T_{\lambda 600}$ and GM1-$T_{\lambda 600}$, showing in both cases a strong uptake of $T_{\lambda 600}$ after 5 and 60 minutes, compared to their controls (DMSO and GM1, respectively). LNCaP cells were also incubated with $T_{\lambda 600}$ and GM1-$T_{\lambda 600}$ after 2 hours of dialysis and imaged by confocal microscopy, with only dialyzed GM1-$T_{\lambda 600}$ showing cellular internalization of $T_{\lambda 600}$ (bottom panels). Scale Bar = 70 μm. **c.** Flow cytometry of $T_{\lambda 600}$ (red)- and GM1-$T_{\lambda 600}$ (blue)-treated LNCaP cells. A similar signal is observed in both groups after 5 and 60 minutes of stimulation, compared to vehicles DMSO (orange) and GM1 (green), respectively. After the 2-hour dialysis procedure, only cells treated with dialyzed GM1-$T_{\lambda 600}$ (blue histogram in the bottom panel) display a significant signal compared to $T_{\lambda 600}$-stimulated cells

Fig. 4: Testosterone-loaded GM1 micelles (GM1-T) induce specific activation of genomic androgen signaling *in vitro*

Western blot of AR in LNCaP cells (**a**) and rPSC (**b**) treated with ascending concentrations of testosterone (T) or GM1-T for 24 hours. Both, T and GM1-T exhibit the highest effect at a concentration of 10^{-8}-10^{-7} M, which correlates with the physiological concentration of the hormone. AR expression was quantified and normalized to ACTB as the loading control. Treatments are normalized to vehicles and are summaries of three independent experiments. mRNA expression of *PSA* (**c**) and *TMPRSS2* (**d**) in LNCaP cells stimulated for 8 hours with T ($1x10^{-8}$ M), GM1-T ($1x10^{-8}$ M), or their vehicles (DMSO and GM1, respectively). *GAPDH* expression was used as loading control. (*p<0.05 vs. DMSO; #p<0.05 vs. GM1, n=3, ANOVA-Tukey). **e**. Western blot of AR in cytoplasmic and nuclear fractions of LNCaP cells stimulated with T ($1x10^{-8}$ M) or GM1-T ($1x10^{-8}$ M) for 24 hours.

Higher levels of AR in the nuclei were observed in T and GM1-T compared to their vehicles. ACTB and PARP1 were used as loading controls; uncropped membranes are illustrated in Suppl. Fig. 4.

Fig. 5: Androgenic effects induced by GM1-T restore prostate size after castration

a-c. Male Albino Swiss mice were castrated and 6 days later treated with i.p. injections of testosterone (T), GM1-T, or vehicles (EtOH or GM1 respectively) every 12 hours for 3 days. **a.** Picture of prostate complexes from the different groups, denoting bigger sizes in T and GM1-T treated mice. **b.** Weight of prostatic complexes exhibiting a similar recovery after T and GM1-T treatments, compared to sham-operated animals. (***p<0.001 vs. etOH; ###p<0.001 vs. GM1, n=4, ANOVA-Tukey). **c.** Hematoxylin and eosin staining showing columnar epithelial cells (E) and abundant secretion in the acinar lumen of ventral prostates in T and GM1-T. On the contrary, atrophic acini devoid of luminal secretion are observed in vehicle-treated mice. Scale Bar = 100 μm. **d.** Proliferation measured by BrdU incorporation in rPSC *in vitro* after stimulation with testosterone (T, $1x10^{-8}$ M), GM1-T ($1x10^{-8}$ M) or their vehicles for 24 hours, showing a similar percentage of proliferation between T and GM1-T. This result demonstrates that GM1-T is able to increase cell proliferation which contributes to regeneration of the prostate after castration. (*p<0.05 vs. DMSO; #p<0.05 vs. GM1; n=3, ANOVA-Tukey)

Fig. 6: Stimulation with testosterone-loaded micelles avoids activation of MIAS

a. rPSC were stimulated with T ($1x10^{-8}$ M), GM1-T ($1x10^{-8}$ M), T-BSA ($1x10^{-8}$ M) or their vehicles for 30 minutes and analyzed by western blot for phosphorylated ERK1/2

(pERK1/2) as a parameter of MIAS. Results demonstrate MIAS activity after T or T-BSA treatment but absence of MIAS after GM1-T treatment. **b**. LNCaP cells were stimulated with T ($1x10^{-8}$ M), GM1-T ($1x10^{-8}$ M), T-BSA ($1x10^{-8}$ M) or their vehicles for 30 minutes and analyzed by western blot for phosphorylated Akt (pAkt) as a parameter of MIAS. As shown in **a**, GM1-T is unable to induce MIAS. pERK1/2 and pAkt expression were quantified and normalized to ERK or ACTB respectively as the loading controls. Treatments are normalized to their controls and are summaries of three independent experiments; uncropped membranes are illustrated in Suppl. Fig. 4. **c.** Proliferation determined by BrdU incorporation of rPSC stimulated with GM1-T, T-BSA or their vehicles for 24 hours. The MIAS-specific inducer T-BSA ($1x10^{-8}$M) displayed a 2-fold increase in cell proliferation compared to vehicle and GM1-T. (*p<0.05 vs. GM1; #p<0.05 vs. BSA and GM1-T, n=3, ANOVA-Tukey).

Supplementary Figures

Supplementary Fig. 1: Representative TEM images of testosterone-loaded GM1 micelles incubated at different pH. The histograms next to each picture show the frequency of micellar size under each condition. Scale bar = 100nm

Supplementary Fig. 2: cell proliferation determined by BrdU incorporation of primary cultures of HPSC stimulated for 24 hours with increasing concentrations of T or GM1-T. Cells exhibited a similar increase in cell proliferation after both stimuli, which is statistically significant at concentration of $1x10^{-7}$ M and $1x10^{-8}$M (*p<0.05 vs. DMSO o GM1; n=3, ANOVA-Tukey).

Supplementary Fig. 3: Proliferation determined by immunocytochemistry of Ki67 of HPSC stimulated with testosterone (T, $1x10^{-8}$ M), T-BSA ($1x10^{-8}$ M) or their vehicles for 24 hours. T-BSA induces higher proliferation than both vehicle and T treated cells, evidencing the uncontrolled proliferation induced by MIAS. (*p<0.05 vs. vehicle or T, n=3, ANOVA-Tukey).

Supplementary Fig. 4: Original uncropped western blot hyperfilms along with their corresponding Ponceau-S-stained membranes, which were rearranged for the figures of the manuscript.

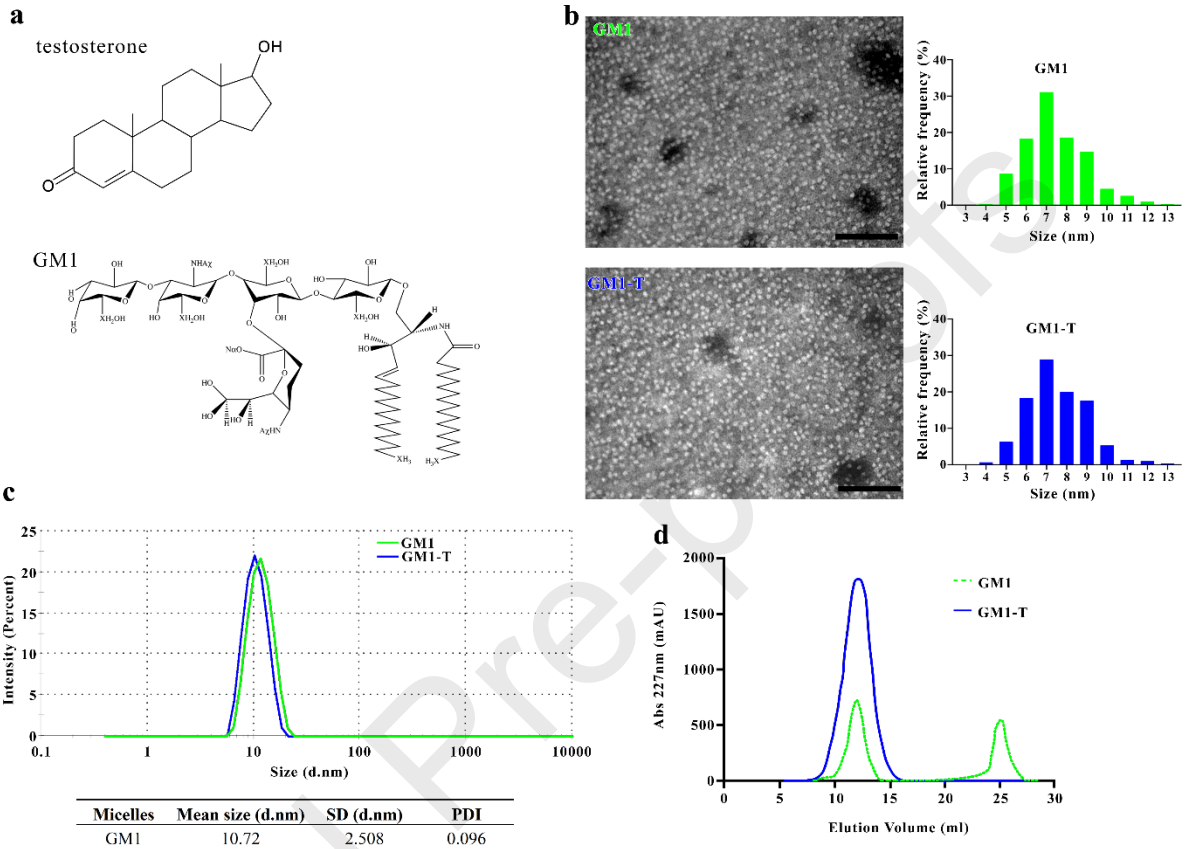

Micelles	Mean size (d.nm)	SD (d.nm)	PDI
GM1	10.72	2.508	0.096
GM1-T	11.92	2.960	0.025

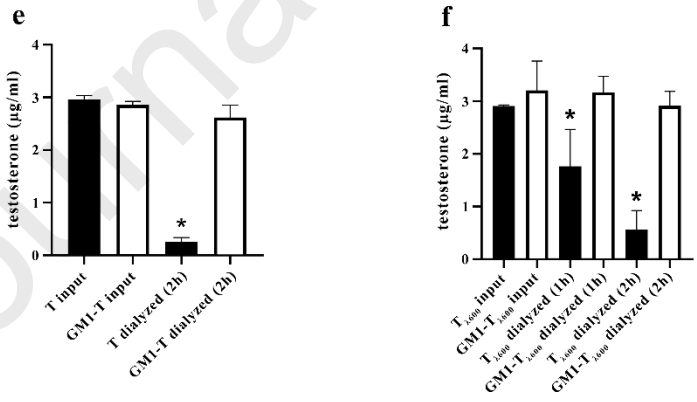

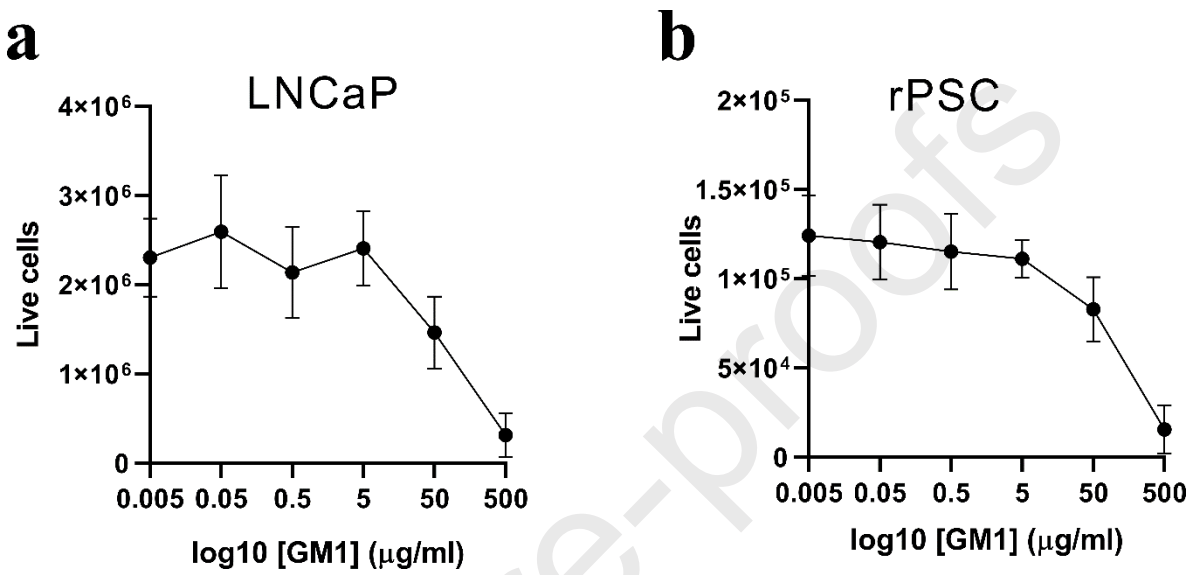

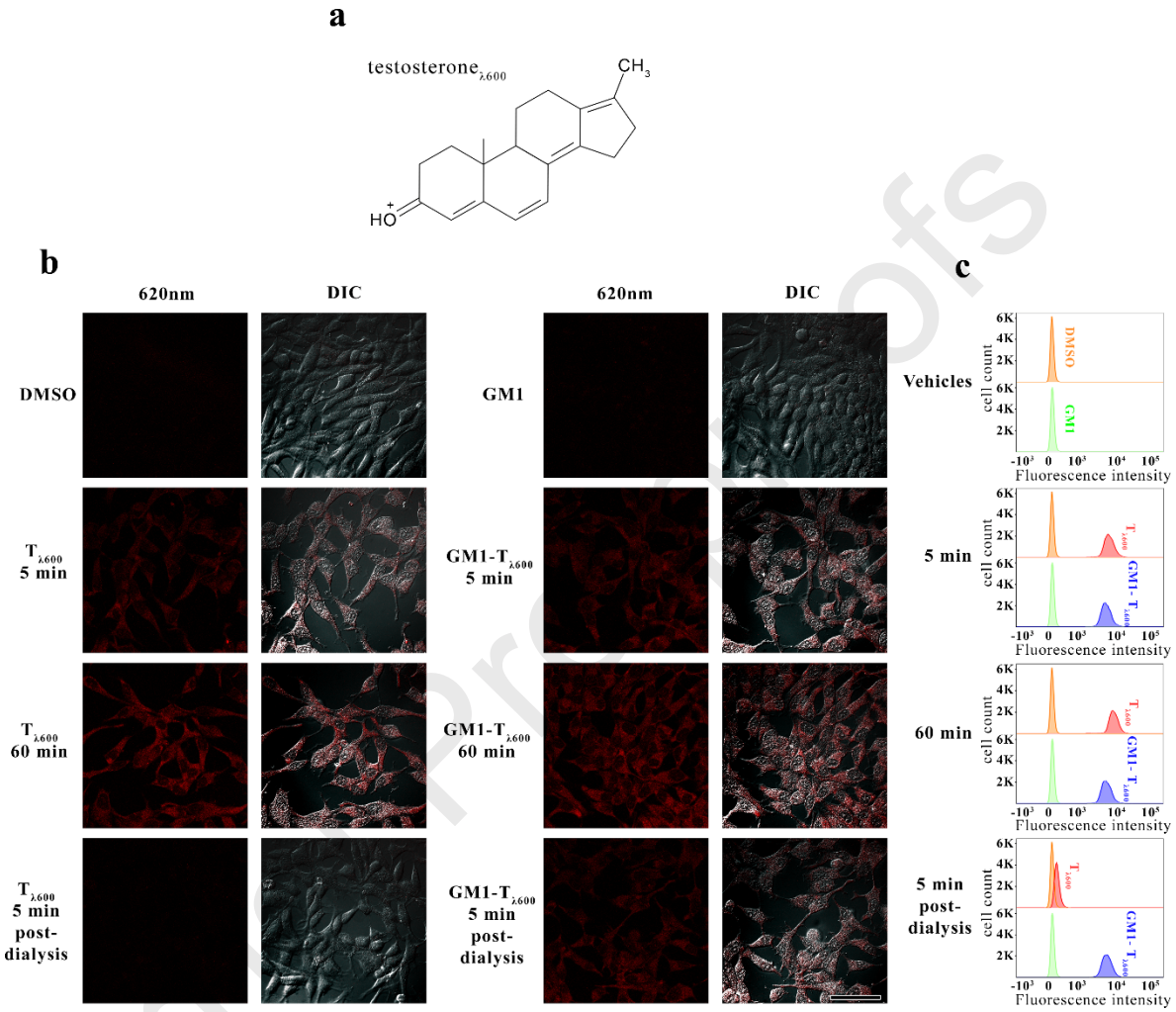

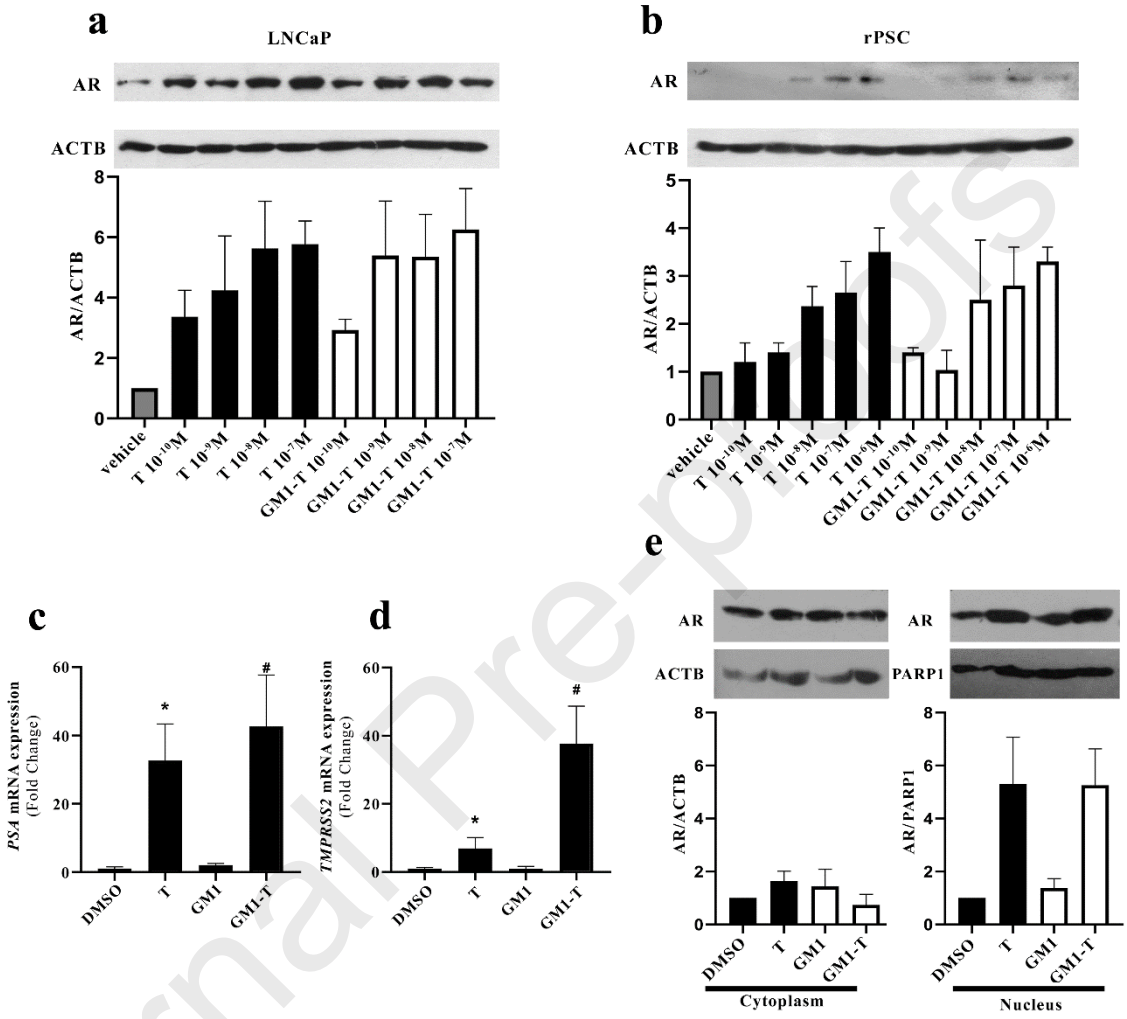

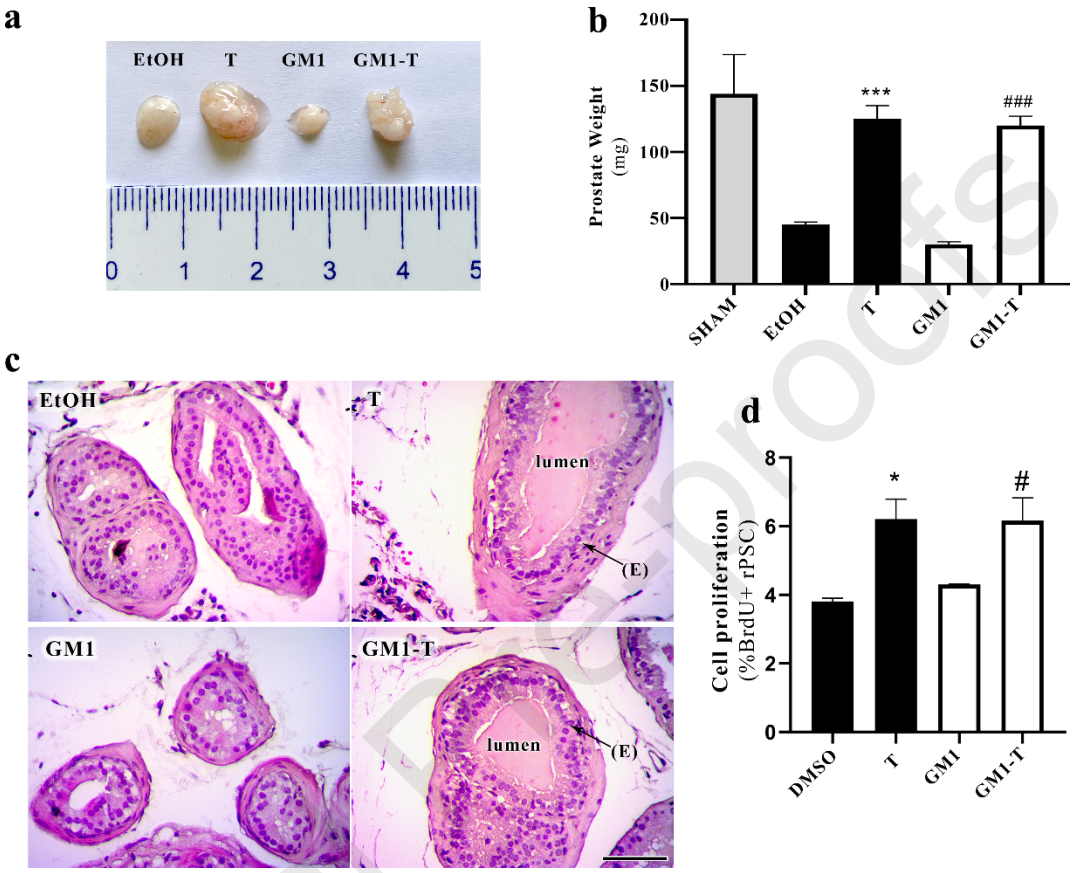

Highlights

- Testosterone can be loaded into GM1 micelles for delivery into the cytoplasm.
- Testosterone-loaded micelles are specific modulators of genomic androgen signaling.
- Genomic signaling can counteract the uncontrolled proliferation induced by MIAS.
- GM1 nanoparticles are efficient tools for specific targeting of steroid receptors.

Graphical abstract

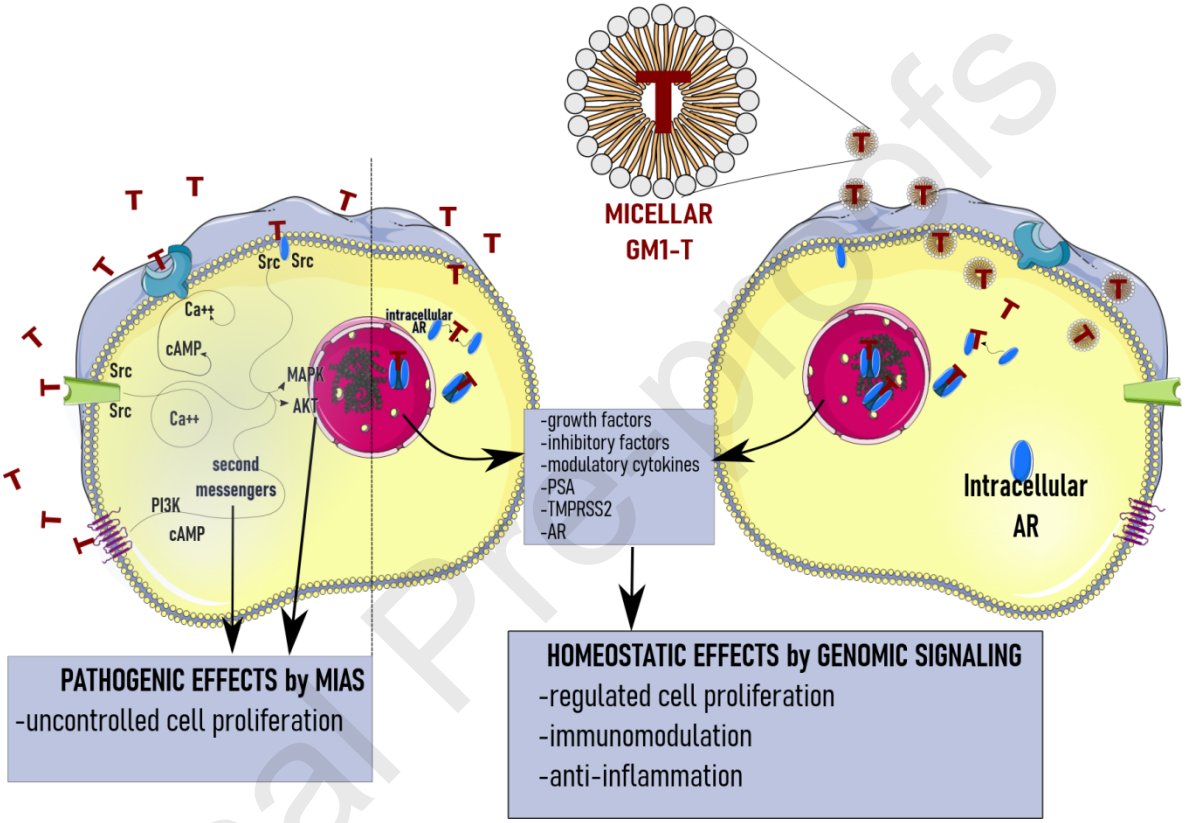

Authors' contributions

N.P.: Conceptualization, Methodology, Validation, Formal analysis, Data acquisition, Writing, Visualization; M.M.C.R.: Data acquisition, Formal analysis; L.D.V.S.: Data acquisition, Methodology, Formal analysis; M.V.S.: Data acquisition, Formal analysis; V.P.: Data acquisition, Formal analysis; J.P.N: Data acquisition, Methodology, Formal analysis; R.V.A.: Data acquisition, Formal analysis; D.M.B.: Conceptualization, Methodology; A.A.Q: Conceptualization, Methodology, Writing, Visualization, Supervision, Project administration, Funding acquisition; C.A.M.: Conceptualization, Methodology, Writing, Supervision, Project administration, Funding acquisition. All authors read and approved the final manuscript.

Declaration of interests

☒ The authors declare that they have no known competing financial interests or personal relationships that could have appeared to influence the work reported in this paper.

☐The authors declare the following financial interests/personal relationships which may be considered as potential competing interests: